

# Loosely Coupled Payload Transport System with Robot Replacement

Pulkit Verma, Rahul Tallamraju, Abhay Rawat, Subhasis Chand, and Kamalakar  
Karlalalem

International Institute of Information Technology, Hyderabad, India  
{pulkit.verma@research., rahul.t@research.,  
abhay.rawat@research., subhasis.chand@research.,  
kamal@}iiit.ac.in

**Abstract.** In this work, we present an algorithm for robot replacement to increase the operational time of a multi-robot payload transport system. Our system comprises a group of non-holonomic wheeled mobile robots traversing on a known trajectory. We design a multi-robot system with loosely coupled robots that ensures the system lasts much longer than the battery life of an individual robot. A system level optimization is presented, to decide on the operational state (charging or discharging) of each robot in the system. The charging state implies that the robot is not in a formation and is kept on charge whereas the discharging state implies that the robot is a part of the formation. Robot battery recharge hubs are present along the trajectory. Robots in the formation can be replaced at these hub locations with charged robots using a replacement mechanism. We showcase the efficacy of the proposed scheduling framework through simulations and experiments with real robots.

**Keywords:** Multi-Robot System · Operational time · Robot replacement · Optimization.

**Video Link:** <https://youtu.be/-6ivGT3dOQw>

## 1 Introduction

Coordination between multiple robotic agents to collectively perform tasks such as payload transportation [2] [24], search and rescue [10] [9] and area exploration [3] [19], have been a field of interest. Advantages of using multiple robots over a single robot have been well established in certain application domains [4] [13] [25]. Battery life of a robot is a crucial aspect [7] [8] [18] in highly coordinated tasks and applications such as payload transportation. Complete battery discharge of a single robot during payload transportation can render the task incomplete. *In this paper, we focus on robots replacement in a multi-robot payload transport system such that the operational time of the system is well beyond the battery life of an individual robot. Robot replacement ensures that the high-level task of payload transportation remains less dependent on the robot's battery life, we present a battery discharge aware robot replacement mechanism.*

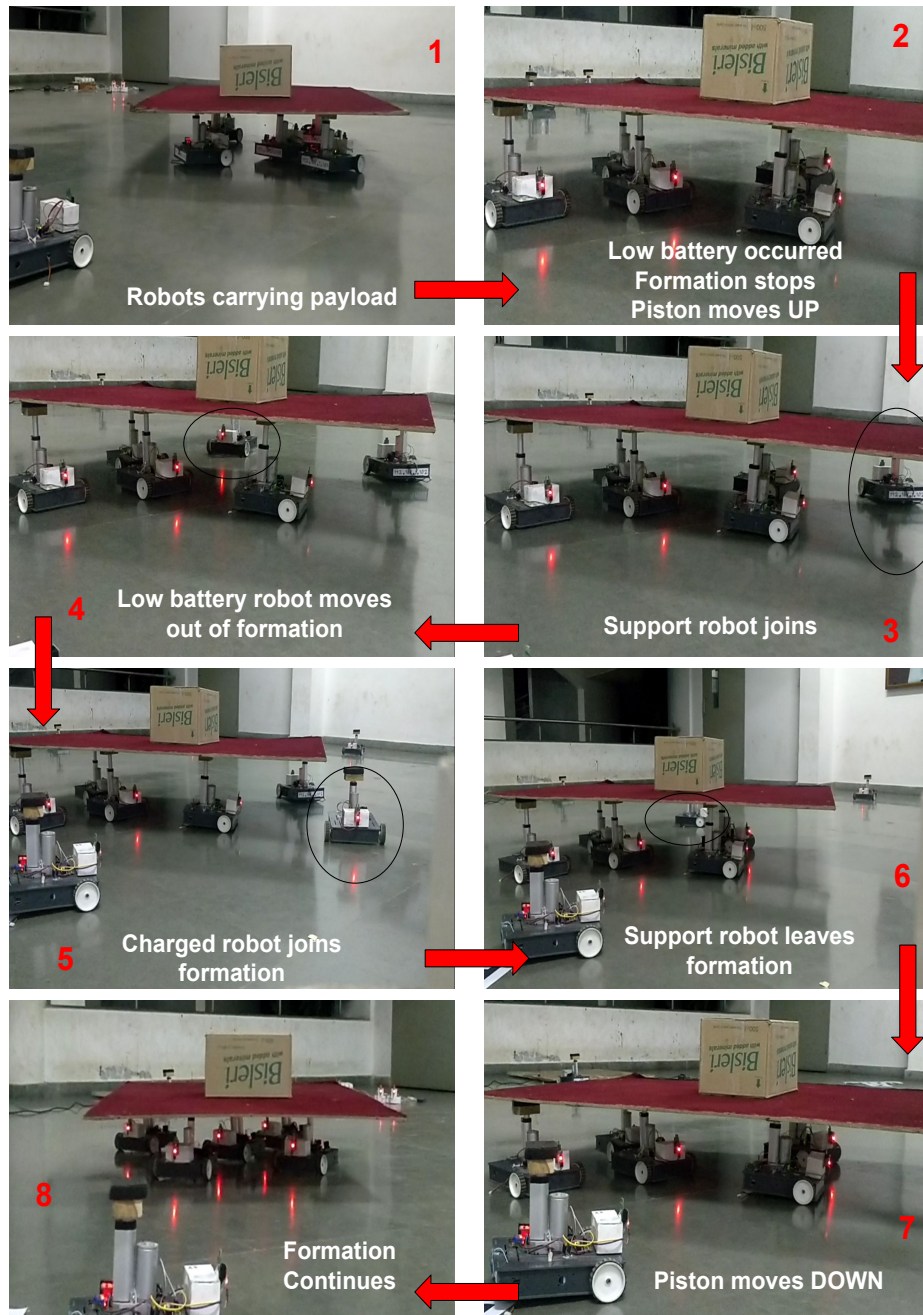


Fig. 1: Robot Replacement Process (for more details, see video at <https://youtu.be/-6ivGT3dOQw>)

In our work, a formation of robots transports payloads. The robots in a formation refer to the robots that are contributing to transporting the payload while the other robots are distributed among the charging stations (or recharge hubs). Recharge hubs are present alongside the trajectory to carry out replacements. The formation carrying the payload traverses along a trajectory used by a leader robot. Other robots in the formation derive their trajectories using a decentralized control law [14] with respect to the designated leader robot. Fully or partially charged robots are present in recharge hubs which are used to replace low battery robots in the formation using our algorithm.

An optimization problem is formulated to (a) extend the operational time of the complete system and (b) reduce the number of replacements while traversing the trajectory, adhering to the system constraints. Fig.1 depicts the series of steps that are followed to carry out a replacement in a formation.

We also demonstrate the hardware results (in Section 5.2) of the presented payload transport system with five robots moving in a formation carrying a payload. A circular trajectory is considered with two recharge hubs on its periphery containing one robot at each hub. Replacements are carried out at any of these hubs as dictated by our algorithm. Robots are equipped with current and voltage measuring circuit which is used to calculate the battery consumption of each robot. The consumption data is sent to an optimization solver running on a server. The optimization provides a binary solution vector, where 1 represents robot in a formation and 0 represents robot at recharge hub. We identify the low battery robot(s) and charged robot(s) by using the solution vectors generated at the current and previous recharge hub respectively (refer to 4.1). The replacement of the low battery robots is carried out with charged robots present at the hub without any human intervention. In order to automate robot replacements and maintain payload stability during robot replacements, we utilize *Support Robots*. These are typically present at recharge hubs and are not considered while modeling the optimization.

For physical validation, we consider a payload weighing six kgs. From practical implementation, we observed that the system has an operating time of 40 minutes without any payload and 25 minutes with the payload. Using our proposed robot replacement algorithm, we observe that the operational duration of the system increases by about 20 minutes i.e. the operating time is increased to nearly 1 hour with a payload on them. All the robots in a formation are left with minimal battery after an hour and hence replacement cannot be made as the robots available on the hubs are limited in our case. Increasing the number of robots at the hubs will result in a further increase in the operational time of the system. Note that there is no limit for carrying out the number of replacements i.e. we can make multiple replacements at any hub even if more than one low battery robot is present in the formation, provided enough robots are present at the recharge hub for replacement. However, the multiple replacements are carried out one at a time to avoid instability of the payload. To avoid a long wait time and to showcase the replacement process, the battery threshold for replacement is set to 11.5 volts (having a maximum voltage of 12 volts). If there are no charged robots present at the hub for the replacement(s) of a low battery robot(s), the formation will stop and wait for the replacement robot to be available<sup>1</sup>.

<sup>1</sup> Video at: <https://youtu.be/-6ivGT3dOQw>

Some assumptions are made to showcase the efficacy of presented solution on real robots:

- The robots are moving on flat terrain. Inclined planes are not considered in this paper.
- The battery in each robot is fault free and has an error free charging and discharging cycle.
- Only low battery faults are considered at this time and no other robot faults like wheel failure, piston failure, etc are considered in this paper.
- As robot replacements typically happen near recharge hubs, we assume that the support robots are always available during robot replacements.

## 2 Related Work

Cooperative payload transport and manipulation using multiple robots has been studied before [24] [2] [17]. However, to the best of our knowledge, none of the approaches consider maximizing operational time of a loosely coupled formation of robots for payload transportation. Therefore, we review literature related to different aspects of our work. Battery aware approaches to plan and control, use battery models as constraints to improve the run time of the system. [18] [27] solves the multi-agent rendezvous problem using constraints on robot kinematics and battery. Time of flight of drones is maximized by using mobile ground recharge stations to charge the drones during real-time operations [8]. While we consider maximization of operational time in our work, we plan for the formation of mobile robots with task constraints to transport a common payload. In [16], the robots are used for area exploration in an unknown environment and recharge them on charging points present at a fixed location. The author considers the battery parameter for charging and discharging but does not deal with the replacement of robots. Battery is shared among robots [11] [12] [26], where each robot has multiple battery packs. The batteries can optionally be shared on-the-go with other robots in the vicinity, which are running low on battery charge. Even though the authors solve the issues of increasing system lifetime by increasing the number of batteries, but the approach, however, involves extra effort to carry additional battery weight. In our approach, we use a single battery robot and recharge them when running low on charge. However, this can be extended to multiple batteries on a single robot.

The concept of working robots in the home area and foraging area is discussed in [1], where the robots in the home area move to perform a task and robots in a foraging area search for known or unknown power stations. As the power of the robots in the home area is reduced to a certain threshold, the forage robots help them to find the nearest power station. Though the author deals with recharging the robots and increasing the battery life but does not deal with robot replacement in the formation of robots. Time and energy constrained schedules have been generated for multiple robotic manipulators using a mixed integer nonlinear program [23]. Parameters like battery models and component power consumption were considered [7] for effective long-term power management in a socially constrained multi-robot system. Failure resilient multi-agent system is considered in [21] where a robot with multiple wheels is used to carry a payload. The author deals with minimizing the energy of the system and maximizing the

traveled distance by switching on and off the motors (agents) such that the robot trajectory remain unaffected. While the aforementioned works study battery constrained planners and schedulers, they do not deal with the task of formation, payload and battery constrained multi-robot systems.

### Contribution and Organization

In our work, the robots are given a task of transporting a payload. In this paper, we present an algorithm for task constrained optimal robot replacement to extend the operational time of a multi-robot system. We formulate an optimization problem to determine the set of discharged robots, which have to be replaced by charged robots from a recharge hub. Our optimization is a quadratic program which is constrained by (a) the number of robots required to transport the payload, (b) the battery levels of each robot in the formation and (c) battery levels of robots at recharge hub stations. The nature of the modeled optimization problem is quadratic as the voltage of the robot reduces quadratically with the number of time steps. (see equation 11). We discuss the battery discharge of a Li-Ion battery and consider kinodynamics of the non-holonomic differential drive robot to simulate and implement our algorithm. The replacement of the low battery robot with a charged robot is presented using our algorithm. However, to the best of our knowledge, no previous work has been done on extending the operational time of a multi-robot system for the task of payload transportation (considering non-holonomic wheeled mobile robots) using robot replacement.

We discuss the kinematics, dynamics and battery model of a differential drive robot in Section 3. We discuss about modeling an optimization problem to find the charged and low battery robots at a hub and in the formation respectively in Section 4. The section also describes a replacement strategy to replace low battery robots with charged robots. To make our solution more concrete, we display simulation and experimental results in Section 5. Conclusion and future scope is discussed in Section 6

## 3 Modeling and Control

This section deals with a discussion on kinematics, dynamics, and frictional model, followed by a battery model of each robot and an approach for making multiple robots to move in a loosely coupled formation.

### 3.1 Kinematics Model

A nonholonomic robot is considered, with generalized coordinates  $\mathbf{q} = [x, y, \theta, \phi_r, \phi_l]^T$ , where  $(x, y)$  is the position in the inertial frame and  $\theta$  is the yaw angle,  $\phi_r$  and  $\phi_l$  represent the angular positions of the left and right wheel. The evolution of generalized coordinates with is given by the following equation.

$$\begin{aligned} \dot{\mathbf{q}} &= \mathbf{S}(\mathbf{q})\boldsymbol{\nu} \\ \text{where, } \boldsymbol{\nu} &= [v \ w]^T \end{aligned} \quad (1)$$

and  $\mathbf{S}(\mathbf{q})$  spans the null space of the non-holonomic constraint matrix of the differential drive robot.  $v$  and  $\omega$  are robot's pseudo linear and angular velocity control inputs.

### 3.2 Dynamics Model

The dynamics equation for the considered differential drive robot are derived using the Euler-Lagrange formulation [15].

$$\begin{aligned} M(\mathbf{q})\dot{\phi} + \mathbf{m}(\mathbf{q}, \phi) &= \mathbf{G}^T(\mathbf{q})\mathbf{S}(\mathbf{q})\boldsymbol{\tau} \\ M(\mathbf{q}) &= \mathbf{G}^T(\mathbf{q})\mathbf{B}(\mathbf{q})\mathbf{G}(\mathbf{q}) \\ \mathbf{m}(\mathbf{q}, \phi) &= \mathbf{G}^T(\mathbf{q})\mathbf{B}(\mathbf{q})\dot{\mathbf{G}}(\mathbf{q})\phi + \mathbf{G}^T(\mathbf{q})\mathbf{C}(\mathbf{q}, \dot{\mathbf{q}}) \end{aligned} \quad (2)$$

$\mathbf{G}(\mathbf{q})$  is the transformation matrix,  $\mathbf{B}(\mathbf{q})$  is a symmetric positive definite inertia matrix,  $\mathbf{C}(\mathbf{q}, \dot{\mathbf{q}})$  is the Coriolis matrix. Also,  $\boldsymbol{\tau} = [\tau_r \ \tau_l]^T$  where,  $\tau_r, \tau_l$  are the torques generated by the right and left wheels respectively.

### 3.3 Battery Model

Each robot in our system is equipped with a Li-Ion battery. The discharge profile of a typical Li-Ion battery with a capacity of  $1200mAh$  is empirically obtained and an analytical model is developed through curve fitting [22]

$$VI^n(D) = \frac{(a_1 + a_3D + a_5D^2)}{(1 + a_2D + a_4D^2 + a_6D^3)} \quad (3)$$

where, variables  $a_1, a_2, \dots, a_6$  are coefficients determined by least squares curve fitting,  $VI^n$  represents the voltage discharge ( $D$ ),  $n$  is a constant ( $\approx 0.005$ )<sup>2</sup>. The voltage during discharge is found using the below equation.

$$V_t = \frac{I^n V(D)_{t-1}}{I_t^n} = \left( \frac{I^n V(D)_{t-1}}{P_e^n} \right)^{\frac{1}{(1-n)}} \quad (4)$$

where,  $I_t = \frac{P_e}{V_t}$ ,  $P_e$  is the electrical power,  $I_t, V_t$  are the current and voltage at time instant  $t$ . The discharge capacity for the next discrete time step is the summation of the present battery capacity and the discharge for a  $\Delta t$  time interval.

$$D_t = I_t(\Delta t) + D_{t-1} \quad (5)$$

Electrical power  $P_e$  for each differential drive robot is also given by

$$P_e = \frac{\tau_i \dot{\phi}_i}{\eta}, \quad i \in \{\text{left wheel, right wheel}\} \quad (6)$$

$\eta$  is robot's motor efficiency. The generated torque per motor  $\tau_i$  and the current  $I_{w,i}$  per motor is given as,

$$\tau_i = K_t(I_{w,i} - I_0) - b\dot{\phi}_i, \quad I_{w,i} = \frac{V_i - K_e\dot{\phi}_i}{R} \quad (7)$$

<sup>2</sup> For detailed battery model, Refer [22].

$I_0$ ,  $K_t$ ,  $R$ ,  $K_e$ ,  $b$  are the no-load current, torque constant, internal resistance, back-emf constant and damping constant of the DC motor respectively.

Substituting the actuator torque and current equation (7) in dynamics equation (2) we obtain the integrated motor, battery and robot dynamics equations which are used to estimate the robot battery discharge where the discharge is directly proportional to the mass. Fig.2 presents the battery voltage and discharge curves plotted against time for different mass values. The solid lines represent the voltage curves whereas the dotted lines represent the discharge curves. From the figure, it is clear that discharge curves are steeper for heavier payload. The black dotted lines show the discharge at 30% and 40% remaining battery level.

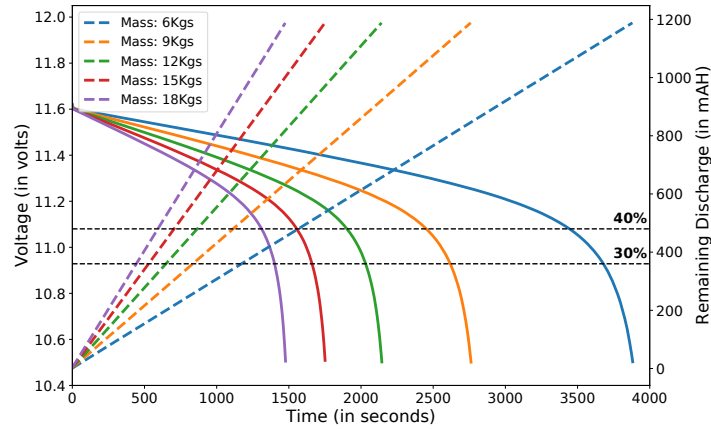


Fig. 2: Voltage vs Time plot at different Mass of Payload

### 3.4 Formation Control

We implement a decentralized leader-follower formation control law. A leader robot is assigned a predefined closed loop trajectory, generated from a global motion planner [20]. All other robots derive their respective pseudo command velocities from the leader's position and command velocities. Fig.3 shows the graphical representation of the information flow between the leader and followers. The decentralized control law [14] is given by the following equations.

$$\begin{aligned} v_j &= k_1 \alpha_j + v_i \cos \theta_{ij} - \rho_{ij}^d \omega_i \sin(\psi_{ij}^d - \theta_{ij}) \\ \omega_j &= (v_i \sin \theta_{ij} + \rho_{ij}^d \omega_i \cos(\psi_{ij}^d + \theta_{ij}) + k_2 \beta_j + k_3 \theta_{je}) / d \end{aligned} \quad (8)$$

where  $\alpha_j$  and  $\beta_j$  is the error in longitudinal and vertical direction respectively which is given by

$$\begin{aligned}\dot{\alpha}_j &= -k_4\alpha_j + (k_5 - \alpha_j)f_{1j}(x_{je}) - (k_6 + \alpha_j)g_{1j}(x_{je}) \\ \dot{\beta}_j &= -k_4\beta_j + (k_5 - \beta_j)f_{2j}(y_{je}) - (k_6 + \beta_j)g_{2j}(y_{je})\end{aligned}\quad (9)$$

and

$$\begin{aligned}f_{1j}(x_{je}) &= \text{Max}(k_1x_{je}, 0), & g_{1j}(x_{je}) &= \text{Max}(-k_1x_{je}, 0) \\ f_{2j}(y_{je}) &= \text{Max}(k_2y_{je}, 0), & g_{2j}(y_{je}) &= \text{Max}(-k_2y_{je}, 0)\end{aligned}$$

where constants  $k_1, k_2, k_3, k_4, k_5, k_6 > 0$ ,  $\rho_{ij}^d$  and  $\psi_{ij}^d$  are the desired distance and

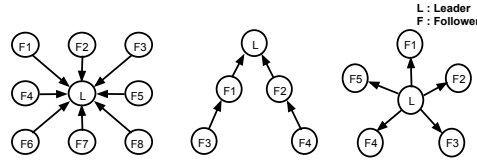


Fig. 3: Leader follower formation with different formation shapes

orientation to maintain between the leader and follower robot,  $v_i$  and  $\omega_i$  are the linear and angular velocities of the leader,  $v_j$  and  $\omega_j$  are the generated linear and angular velocities of the  $j^{th}$  follower,  $d$  is distance from the robot's center to the robot's center of mass.  $\theta_{ij}$  is the orientation error of the leader and follower i.e.  $\theta_{ij} = \theta_i - \theta_j$  where  $\theta_i$  and  $\theta_j$  are the leader and follower orientation respectively.  $x_{je}, y_{je}, \theta_{je}$  are the positional tracking errors between the leader and follower.

Additionally, we constraint the robots in the formation to maintain a minimum distance  $\rho_{ij}^d$ , such that it guarantees that a path always exists for any robot in the formation to move in and move out of the formation. Therefore,  $\rho_{ij}^d$  is determined using the dimension of the robot and an approximate error ( $\delta$ ) in the received localization values from the Decawave modules [5]. From the experimental analysis, we analyzed that the value of  $\delta$  is nearly equal to 0.05 meters.

## 4 Selection Mechanism for Replacement

In section 4.1, a mechanism is proposed to identify the low battery robots in the formation and consequently find the charged robots from the hubs for replacement. The problem is modeled as an optimization which takes the present battery level of all robots as input and decides on the subset of robots in the formation which have to be replaced (or recharged). When the formation reaches a hub, the optimizer numerically computes a solution to replace the low battery robot with a charged robot present at the current hub and identifies the robots to be replaced. A robot replacement strategy is discussed in section 4.2. The sequence of steps involved in the proposed approach is shown below.



---

**Sequence of Steps 1: Robot Selection and Replacement Process**

---

```

1  elect robots to carry a payload
2  Make formation based on shape of the payload
3  Provide trajectory information to the leader
4  Formation starts moving
5  Monitor battery status of all the robots
6  Run Optimization on reaching recharge hubs to get solution vector
7  Check if replacement is needed, based on the solution vector
8  if Replacement then
9      if Replacement available then
          Piston moves up for all the robots
          Support robot joins the formation without colliding with the neighbour robots
          Piston moves up for the support robot
          Piston moves down for the low battery robot
          Low battery robots moves out of the formation and reaches hub
          Charged robot occupies the place vacated by the low battery robot
          Piston moves up for the charged robot
          Piston moves down for the support robot
          Support robot moves out of the formation
          Piston for all the robots in formation moves down
          Go to step 3
        else
          System waits until a replacement is available
10     end
11 else
    Go to step 3
12 end

```

---

**4.1 Battery Discharge based Selection**

In our system, each robot has two states (a) Active state i.e. robot is in the formation and carrying the payload (b) Inactive state i.e. robot is not in the formation and charging its battery. A robot in an active state undergoes continuous discharge whereas in inactive state a robot is charged at a hub. A quadratic program is formulated, in order to make decisions which would *a*) extend the operating time of the formation, *b*) reduce the long-term expected cost of replacing the robots at hubs, adhering to system constraints.

**Optimization Formulation** We model a moving horizon based optimization where we consider a few steps ahead (horizon length) to select a set of robots that contribute to payload transportation. Let  $N$  be the total number of available robots,  $k$  be the horizon length ( $k = 2$  in our work) such that  $k < N_h$ ,  $N_h$  being then total number of recharge hubs. Let  $\mathbf{X}^j$  be a  $N$  length binary vector represented as  $(x_1 \ x_2 \ \dots \ x_N)$ ,  $\mathbf{X}^j$  is the solution vector at  $j^{th}$  hub,  $j = 1, 2, \dots, k$  and  $x_i \in \{0, 1\}$  for  $i = 1, 2, \dots, N$  where  $x_i = '1'$  when  $i^{th}$  robot is active (discharging) and '0' if robot is inactive (charging).  $\mathbf{D}^j$  be a  $N$  length vector written as  $(d_1 \ d_2 \ \dots \ d_N)$  which is the discharge vector at  $j^{th}$  hub,  $d_{min} \leq d_i \leq d_{max}$ ,  $d_i$  corresponds to the battery consumption of the  $i^{th}$  robot

(in mAh), where  $d_{min}$  means fully charged robot (0 mAh consumed) and  $d_{max}$  denotes completely discharged robot (1200 mAh consumed).

The estimated battery discharge vector for the robots at  $m^{th}$  horizon ( $m < k$ ) is given by

$$\mathbf{D}^{m+1} = \mathbf{D}^m + r_d \mathbf{X}^m + r_c (1 - \mathbf{X}^m) \quad (10)$$

where  $r_c, r_d$  are predetermined charge and discharge constants between any two consecutive hubs respectively. The more generalized form of the above equation can be written as

$$\mathbf{D}^m = \mathbf{D}^0 + m r_c + (r_d - r_c) \sum_{j=1}^m \mathbf{X}^j \quad (11)$$

where  $\mathbf{D}^0$  is the initial discharge vector. We minimize the battery discharge of the robots in formation at the  $k^{th}$  hub, to ensure longer operational time of the complete system. Using Equation(11), we can write the discharge of active robots at  $k^{th}$  hub as  $(\mathbf{D}^k)^T \mathbf{X}^k$ .

Note, higher the number of replacements made at any hub point, the more time system remains idle, causing delay in the transportation. Therefore, we also maximize the robot retention at any recharge hub, i.e. to keep the same robots in formation, which ensures carrying out minimum number of replacements at a hub point. Let  $\mathbf{H}^j$  be a  $N$  length binary vector represented as  $(h_1^j \ h_2^j \ \dots \ h_N^j)$  for  $j^{th}$  hub,  $h_i \in \{0, 1\}$  for  $i = 1, 2, \dots, N$  and  $j = 0, 1, \dots, N_h - 1$ .  $h_i^j = '1'$  if  $i^{th}$  robot is present at the  $j^{th}$  hub and '0' otherwise. Here, retention refers to using a robot for two consecutive state vectors (hubs). Hence, the retention of robots ( $\mathbf{R}_r$ ) for  $k$  horizons is written as

$$\mathbf{R}_r = \sum_{j=1}^k \mathbf{X}^j \mathbf{X}^{j-1} \quad (12)$$

The optimization can now be modeled as a quadratic program as shown below:

$$\text{minimize } \frac{1}{2} \mathbf{X}^T \mathbf{P} \mathbf{X} + \mathbf{Q}^T \mathbf{X} \quad (13)$$

subject to: *Formation Constraint* (14)

*Battery Constraint* (15)

*Hub Constraint* (16)

where  $\mathbf{X} = (\mathbf{X}^0 \ \mathbf{X}^1 \ \dots \ \mathbf{X}^k)^T$  is  $kN \times 1$  length optimization vector.  $\mathbf{P}$  is a  $kN \times kN$ -dimension real symmetric matrix,  $\mathbf{Q}$  is a  $kN \times 1$ -dimension real valued vector.

$$\mathbf{P} = w_1 \mathbf{P}_d - w_2 \mathbf{P}_r$$

$$\mathbf{Q} = w_1 \mathbf{Q}_d - w_2 \mathbf{Q}_r$$

$P_r, P_d$  are the Quadratic terms in the objective denoting the coefficients of robot retention and battery discharge respectively. Here  $\otimes$  refers to the Kronecker product.

$$P_r = \begin{bmatrix} 0 & 1 & 0 & \cdots & 0 & 0 \\ 1 & 0 & 1 & \cdots & 0 & 0 \\ 0 & 1 & 0 & \cdots & 0 & 0 \\ \vdots & \vdots & \vdots & \ddots & \vdots & \vdots \\ 0 & 0 & 0 & \cdots & 0 & 1 \\ 0 & 0 & 0 & \cdots & 1 & 0 \end{bmatrix}_{k \times k} \otimes I_{N \times N}, \quad P_d = \begin{bmatrix} 0 & 0 & \cdots & 1 \\ 0 & 0 & \cdots & 1 \\ \vdots & \vdots & \ddots & \vdots \\ 1 & 1 & \cdots & 2 \end{bmatrix}_{k \times k} \otimes I_{N \times N}$$

$Q_r, Q_d$  are the linear terms of the objective referring to the coefficients of robot retention and battery discharge respectively.

$$Q_r = [1 \ 0 \ 0 \ \cdots \ 0 \ 0]_{1 \times k}^T \otimes \mathbf{X}^0,$$

$$Q_d = [0 \ 0 \ 0 \ \cdots \ 0 \ 1]_{1 \times k}^T \otimes (\mathbf{D}^0 + kr_c)$$

Equation (13) is therefore a result of weighted sum of two objectives where  $w_1, w_2$  are the weights given to each objective.

The **formation constraint** limits the number of robots which can participate in payload transportation, given as

$$\mathbf{C}\mathbf{X}^j = F \quad \forall j = 0, 1, \dots, k \quad (14)$$

where  $F$  is a scalar, denoting number of robots in formation,  $\mathbf{C} = \mathbf{1}_{1 \times N}$ . This will ensure that only  $F$  number of robots are present in the formation.

The **battery constraint** ensures that at each hub, the battery of each robot in the formation is above a certain threshold capacity ( $d_{th}$ ). Using Equation (11), we can model the battery constraint as

$$d_i x_i \leq d_{th} \quad \forall i = 0, 1, \dots, N \quad (15)$$

The **hub constraint** helps in choosing only those robots for the replacements which are available at the current hub. At any horizon, the number of robots retained and the number of robots replaced at the current hub, must sum to the number of robots in a formation. This can be written as

$$(\mathbf{X}^{j-1} + \mathbf{H}^{j-1})^T \mathbf{X}^j = F \quad \forall j = 0, 1, \dots, k \quad (16)$$

The quadratic optimization is solved using CPLEX solver. The optimization takes the robots' battery parameters (measured voltage and current values) as input and generates a binary solution vector. The solution vector generated at the current hub and the previous hub are compared to find the robots to be replaced. The index of each element of the solution vector corresponds to robot id. For e.g. considering ten robots in total and three robots in formation, let the solution vector at the previous hub be

$[1\ 0\ 0\ 1\ 0\ 1\ 0\ 0\ 0\ 0]$  which represents the robots with id  $\{1, 4, 6\}$  were in formation before reaching the current hub. And let the solution vector at current hub after optimization be  $[0\ 1\ 0\ 1\ 0\ 1\ 0\ 0\ 0\ 0]$  which represents the robots with id  $\{2, 4, 6\}$  should be in formation. We therefore see that the robot with id 1 (low battery robot) needs replacement with robot with id 2 (charged robot).

## 4.2 Robot Replacement

In the previous subsection, we discussed the optimization formulation in detail. Numerically evaluating the quadratic integer program, identifies the robots in a formation which have to be replaced with charged robots at a recharge hub. We need to make sure that the payload on top of the robots must not be affected during robot replacement. To facilitate robot replacements, a piston is mounted on each robot to move the payload up and down in case of any failure. When a battery failure occurs, the piston on all the robots moves up to push the payload such that a new robot can join the formation. To ensure payload stability, support robots are utilized to temporarily balance the system until the robots are replaced. The low battery robot moves its piston down and leaves the formation to recharge its battery at the hub. A charged robot (solution provided by the optimization) from the hub reaches the formation and occupies the space vacated by the low battery robot. The piston of the charged robot moves up, such that the support robot can now leave the formation. The support robot lowers down its piston and moves out of the formation. And hence the formation starts traversing its trajectory again. This completes the replacement process.

Collision-free path planning of robots from recharge hub to the formation and vice-versa is done using a global planner [20]. The inter-robot distance is constrained to be greater than the dimensions of a single robot to facilitate robot navigation and replacements. We focus on failure handling of both triangular and rectangular shaped formation for now, but this can be extended to a formation of different shapes. The system can handle any number of replacements at a hub if charged robots are available for replacement at this hub. Also, as the paper deals with a decentralized leader-follower based formation control [14], the replacement criteria remain the same for the leader and followers. When a leader robot loses its battery charge, the id of the new robot (charged robot) is shared with all the followers. The followers then start following the new robot and hence the formation continues. If there is no robot at the hub having sufficient battery for making any replacement or the number of replacement to be carried out is more than the number of robots present at the hub, the optimization fails to compute a solution and the system operation is halted until a replacement is available. In this paper, the idea of robot replacement is carried out to maximize the operating time of the system, however, this replacement mechanism is also applicable in case of other failures in a robot if the localization and mobile capabilities of a robot are not compromised.

## 5 Results

We present simulation and hardware results in this section. Table 1 is a reference to some important parameters and its values, used in the paper.

Table 1: List of Parameters for each robot ( $a_1 - a_6$  are curve fitting gains for battery and  $k_1 - k_6$  are control gains for formation of robots)

Parameter Name	Value
Wheel radius ( $r$ )(in meters)	0.035
Wheel base( $l$ )(in meters)	0.115
$a_1$	12
$a_2$	3.409
$a_3$	39.55
$a_4$	-0.002653
$a_5$	-0.03203
$a_6$	$-8.112e^{-8}$
$k_1$	1.5
$k_2$	1.0
$k_3$	0.025
$k_4$	15.0
$k_5$	1.0
$k_6$	1.0
Torque Const. ( $K_t$ )(in Nm/A)	$28.24 \times 10^{-3}$
Armature resistance(R)(ohms)	2.4
Chassis weight(m)(in Kgs)	1.5
Wheel weight( $m_w$ )(in Kgs)	0.1
Payload weight(in Kgs)	1-18

## 5.1 Simulation Results

The simulation is performed using twelve robots and three recharge hubs. A formation of three robots is continuously traversing a circular trajectory to show the viability of the solution. In the uploaded video<sup>3</sup> we showcased additional hardware results with more number of robots. The average distance of the recharge hubs from the trajectory is around 0.5 meters. The trajectory shape is not limited to a circular path but any random trajectory can be considered to keep the notion of recharge hubs and replacements intact. Three out of twelve robots are used in the formation, while others are distributed over the recharge hubs (excluding the support robots). We introduce and compare our proposed approach to a naive baseline approach. The two approaches include (a) baseline approach, where the robot in the formation get replaced as soon as it loses its battery below a threshold voltage. (b) The second approach is our optimization based approach where we maximize the battery state of robots in the formation for  $k^{th}$  horizon in advance. The simulations are performed at  $k = 2$ . The choice of  $k$  depends on inter-hub distance. If the distance between hubs is large, the value of  $k$  is small typically less than 3. We observed that a high value of  $k$  would violate the constraints in the optimization as some of the robots are completely discharged before reaching the  $k^{th}$  hub point.

<sup>3</sup> Video at: <https://youtu.be/-6ivGT3dOQw>

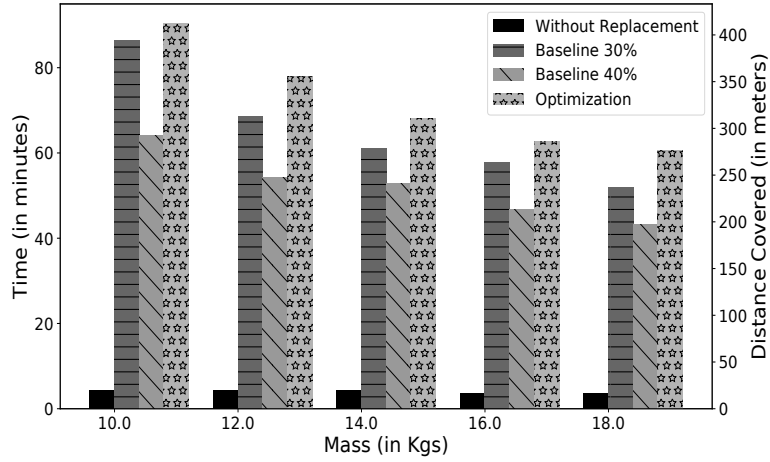


Fig. 4: Payload Operating Time Comparison

Fig. 4 compares the battery life of the two approaches for different weights with a system having no replacement strategy. The robots move in a formation carrying different payload mass. Varying the mass affects robot dynamics which draws a high discharge current and hence increases the battery discharge for heavier mass and vice-versa. Fig. 4 shows that as the mass on the system increases, the battery life of the system reduces. The active time of the system without replacement suffers an early breakdown as there are no robots for replacement. As all the experiments are performed using the same seed value for the initial battery charge (without replacement, baseline, optimization), therefore the distance traveled by the formation without replacement is nearly the same. The system stops as soon as any robots run out of battery. Both baseline and optimization approaches work better than the system without replacement. Also, it can be observed that the baseline approach with threshold level 30% travels more distance than the with 40% battery threshold. Similarly, if the threshold is increased to 60%, the distance traveled by the formation will be even lesser with more number of replacement counts. The optimization on the other hand (the rightmost bar), provides much improved result in terms of increased battery life with a minimal increase in the number of replacements.

Fig. 5 highlights the number of replacements through the lifetime of the system. Each count refers to a robot being replaced at a recharge hub. It is intuitive to think that the robots following the baseline approach (30% threshold) will experience less number of replacements than with (40% threshold), as a robot moves out of formation only if the battery level is below the defined threshold. In the optimized approach, though the robot replacement count is slightly higher, it allows the formation to travel a longer distance (ensuring longer operating time). The replacements are made such that the *Travel time* is more and the total *Replacement Time* is less. Here, *Travel time* corresponds to the

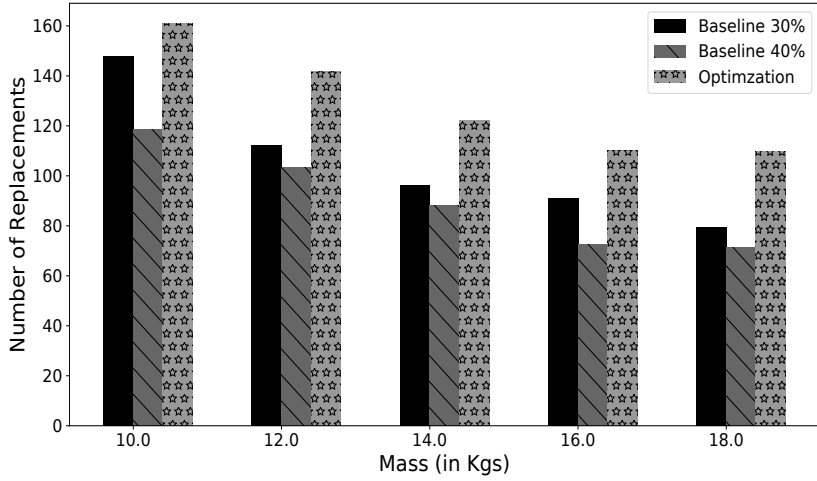


Fig. 5: Total Robot Replacement counts

time utilized in transporting the payload and *Replacement time* is the time taken for replacing the low battery robot with a new one. A balance is maintained between the recharging time and the active time of the battery.

Fig. 6 displays the battery discharge profile for all the robots vs the total hub traversed by the system. *Each robot is displayed with respect to its remaining charge where the dark green shade represents a charged robot that turns lighter as robot discharges. The color turns red if the robot is fully discharged.* It can be seen from the plot that the battery level of the robots (having the same initial battery) is maintained at a higher value in case of optimization than the baseline approach. Hence, the figure shows that the system lasts longer with optimization approach.

One key aspect of the optimization is to note the range of battery's remaining charge when the replacement occurs. Fig.7 shows a comparison of replacement counts with the battery level range for baseline and optimization approach. The baseline approach replaces the robot when the robot battery voltage is less than the threshold battery voltage. The replacement window for 30% battery threshold ranges from 10 – 30% of the total battery charge. This is because of the fact that the robots do not leave the formation even when the battery voltage level is just above the threshold (say 31%), which led the replacements to occur in a threshold window lower than the set threshold. Similarly, with 40% threshold, the replacement window lies in 20 – 40% of total battery range. *However the optimization approach, in comparison to the baseline approach, replaces the robot much before the lowest battery level which allows a robot to recharge itself quickly and thus helps in reducing the charging time of the robot. In optimization, the robot gets replaced even when the battery's remaining charge is in the range of 80 – 90%. As we have modeled our optimization considering future time steps, it some-*

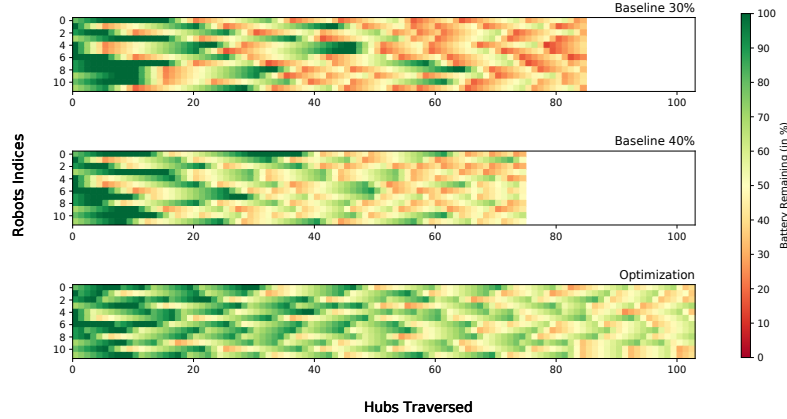


Fig. 6: Battery profile for the robots in formation

*times replaces a charged robot at a particular hub so as to avoid constraint violations, due to the absence of charged robot on the hub.*

Thus, the optimization increases the operational time of the system in comparison to the baseline approach.

## 5.2 Implementation on Robots

The hardware implementation<sup>4</sup> is carried out on a custom built non-holonomic differential drive robots, each having a Raspberry Pi and an Arduino Uno board mounted on it. The robot localization is achieved by fusing the sensor data of Ultra Wide Band transceiver [5] (Decawave DWM1000), robot's wheel odometry and an Inertial measurement unit(IMU-MPU9250), giving a positional accuracy of  $< 6$  cms. We use an extended Kalman filter to fuse information from decawave modules, imu, and wheel odometry to localize the robot. A linear actuator(Piston) is mounted on all the robots to lift the payload up and down to facilitate robot replacement. Each robot can carry a payload weight of around seven kg. All the robots share their information wirelessly on a locally created wifi network. Raspberry Pi does the high level processing such as robot coordination, path planning, etc, with a ROS (Robot Operating System) supported environment. Arduino Uno is used to perform a low level control to execute the command velocities on the robot. It runs PID (Proportional Integral Derivative) control loop to maintain desired wheel velocities of a robot with a loop frequency of 20 Hz. The total cost of each robot is around \$250. PYTHON is used as the programming language to generate the hardware and simulation results.

A total of eight robots were used to perform physical validation with two recharge hubs present at the periphery of the trajectory. Five robots are moving in a formation

<sup>4</sup> Video at: <https://youtu.be/-6ivGT3dOQw>



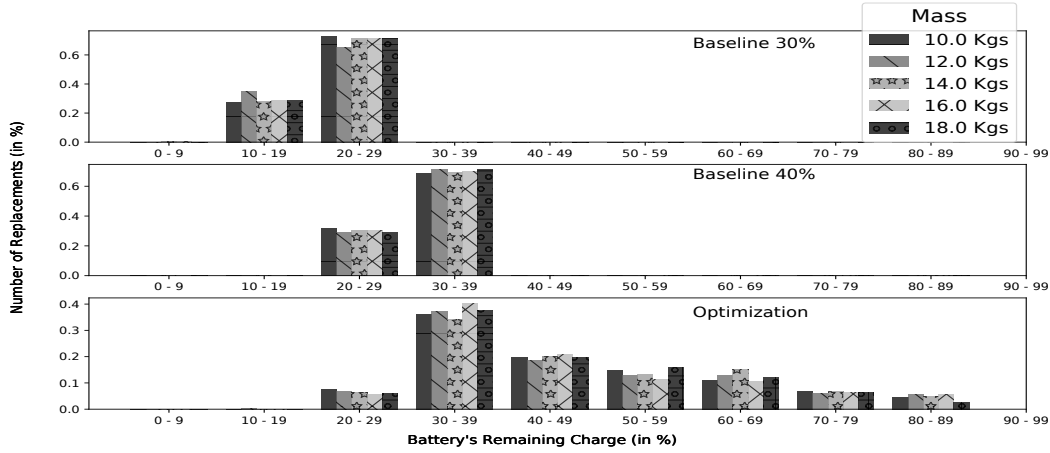


Fig. 7: Replacement Vs Average Battery Discharge

Table 2: Follower desired Distance( $\rho_{ij}^d$ ) (meters) and Angle( $\psi_{ij}^d$ ) (degrees) from the leader

Follower	Parameter	Value
1	$\rho_{ij}^d$	0.6
	$\psi_{ij}^d$	0
2	$\rho_{ij}^d$	0.6
	$\psi_{ij}^d$	90
3	$\rho_{ij}^d$	0.6
	$\psi_{ij}^d$	180
4	$\rho_{ij}^d$	0.6
	$\psi_{ij}^d$	-90

with random initial battery levels and two robots are kept at recharge hubs with nearly full batteries. One support robot is also present on the periphery of the trajectory. The robots were kept in a square formation (four robots at the corners and one in the center). Table 2 contains the values of the desired distance and angle to be maintained by all the followers from the leader. The linear and angular velocity of the robot is  $6 \text{ cms/sec}$  and  $0.05 \text{ radians/sec}$ . Each robot's battery is monitored and shared with the central server which decides on which robot needs to be replaced on the recharge hub (using optimization). CPLEX optimizer by IBM [6] is used to run the optimization. Fig. 1 shows the experimental setup including replacements. After running multiple experiments, we have observed that it takes about 3 minutes for a robot to get replaced at a recharge hub. The complete experimentation has also been implemented and validated on Gazebo simulator.

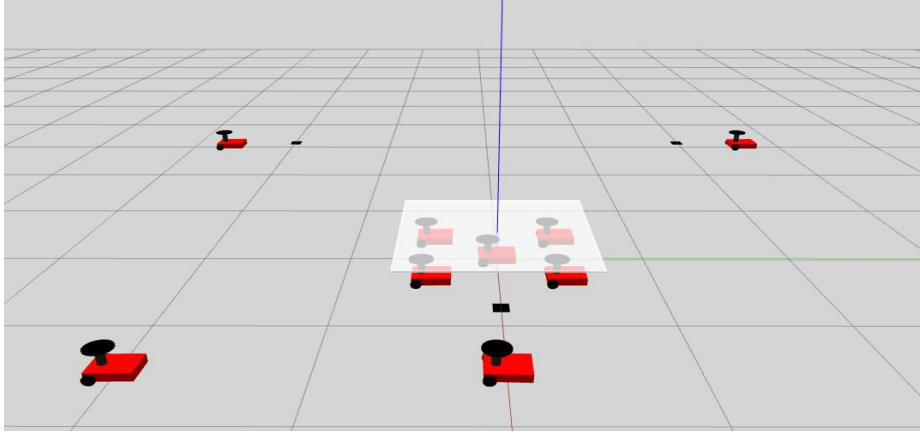


Fig. 8: Experimental Initial gazebo setup: Nine robots are considered in total. Five robots in a formation are carrying a payload. Three recharge hubs, each containing one charged robot, are present along the trajectory. A support robot is also present along the trajectory to assist robot replacement.

Initial set up of the gazebo simulator is shown in Fig.8, where robots move in a circular trajectory containing three hubs. We showcase<sup>5</sup> that the support robot is not always used while replacements are carried out.

## 6 Conclusion

We show the validity of a loosely coupled payload transport system with robot replacement. We built our custom differential drive robots having payload lifting capabilities. The robots carry payload from one place to another while moving in formation and handles any low battery failure in the system to extend the operating time of the system. We presented an algorithm for task constrained robot replacement to increase the operational duration of a multi-robot payload transport system. We formulated an integer quadratic program to identify the low battery robots to be replaced with charged robots to ensure that the system remains operational. The charged robots are present at the recharge hubs that are located on the periphery of the trajectory. Support robots are used in critical replacements where there is a chance unbalanced payloads. We showcased the results of our approach through extensive simulation results and hardware validation results for robot replacement within a formation. Various test cases are considered including multiple replacements at single hub and multiple replacements at multiple hubs. Formations with four robots and five robots carrying payload are showcased undergoing replacements in case of low battery failure.

Future work would involve decentralizing the scheduling algorithms to enable a distributed multi-agent dynamic task allocation. The concept of stationary recharge hubs

<sup>5</sup> Video at: <https://youtu.be/-6ivGT3dOQw>

can be replaced by moving recharge hubs. The present work includes few formation shapes, which can be extended to different formation shapes. Replacing the robots in moving formation can be explored.

## 7 Acknowledgement

The author would like to thank Shrey Agrawal, Ayush Gaud for their help with the physical validation.

## References

1. Ahmad, F.A., Ramli, A.R., Samsudin, K., Hashim, S.J.: Optimization of power utilization in multimobile robot foraging behavior inspired by honeybees system. *The Scientific World Journal* (2014)
2. Alonso-Mora, J., Baker, S., Rus, D.: Multi-robot formation control and object transport in dynamic environments via constrained optimization. *The International Journal of Robotics Research* **36**(9), 1000–1021 (2017)
3. Baranzadeh, A., Savkin, A.V.: A distributed control algorithm for area search by a multi-robot team. *Robotica* **35**(6), 1452–1472 (2017)
4. Cao, Y.U., Fukunaga, A.S., Kahng, A.: Cooperative mobile robotics: Antecedents and directions. *Autonomous robots* **4**(1), 7–27 (1997)
5. Cotera, P., Velazquez, M., Cruz, D., Medina, L., Bandala, M.: Indoor robot positioning using an enhanced trilateration algorithm. *International Journal of Advanced Robotic Systems* **13**(3), 110 (2016)
6. CPLEX, I.I.: V12. 1: User’s manual for cplex. International Business Machines Corporation **46**(53), 157 (2009)
7. Deshmukh, A., Vargas, P.A., Aylett, R., Brown, K.: Towards socially constrained power management for long-term operation of mobile robots. In: 11th Conference Towards Autonomous Robotic Systems, Plymouth, UK (2010)
8. Khonji, M., Alshehhi, M., Tseng, C.M., Chau, C.K.: Autonomous inductive charging system for battery-operated electric drones. In: Proceedings of the Eighth International Conference on Future Energy Systems. pp. 322–327. ACM (2017)
9. Liu, Y., Nejat, G.: Multirobot cooperative learning for semiautonomous control in urban search and rescue applications. *Journal of Field Robotics* **33**(4), 512–536 (2016)
10. Matos, A., Martins, A., Dias, A., Ferreira, B., Almeida, J.M., Ferreira, H., Amaral, G., Figueiredo, A., Almeida, R., Silva, F.: Multiple robot operations for maritime search and rescue in eurathlon 2015 competition. In: OCEANS 2016-Shanghai. pp. 1–7. IEEE (2016)
11. Ngo, T.D., Schioler, H.: A truly autonomous robotic system through self maintained energy. In: Proceedings of the International Symposium on Automation and Robotics in Construction (2006)
12. Ngo, T.D., Raposo, H., Schioler, H.: Potentially distributable energy: Towards energy autonomy in large population of mobile robots. In: Computational Intelligence in Robotics and Automation, 2007. CIRA 2007. International Symposium on. pp. 206–211. IEEE (2007)
13. Parker, L.E., Tang, F.: Building multirobot coalitions through automated task solution synthesis. *Proceedings of the IEEE* **94**(7), 1289–1305 (2006)
14. Peng, Z., Wen, G., Rahmani, A., Yu, Y.: Leader–follower formation control of nonholonomic mobile robots based on a bioinspired neurodynamic based approach. *Robotics and autonomous systems* **61**(9), 988–996 (2013)

15. Ramos, M.T.: Model and control of a differential drive mobile robot (2013), <https://goo.gl/HaXKM>
16. Rappaport, M., Bettstetter, C.: Coordinated recharging of mobile robots during exploration. In: Intelligent Robots and Systems (IROS), 2017 IEEE/RSJ International Conference on. pp. 6809–6816. IEEE (2017)
17. Rus, D., Donald, B., Jennings, J.: Moving furniture with teams of autonomous robots. In: Intelligent Robots and Systems 95.'Human Robot Interaction and Cooperative Robots', Proceedings. 1995 IEEE/RSJ International Conference on. vol. 1, pp. 235–242. IEEE (1995)
18. Setter, T., Egerstedt, M.: Energy-constrained coordination of multi-robot teams. *IEEE Transactions on Control Systems Technology* **25**(4), 1257–1263 (2017)
19. Sharma, S., Shukla, A., Tiwari, R.: Multi robot area exploration using nature inspired algorithm. *Biologically Inspired Cognitive Architectures* **18**, 80–94 (2016)
20. Şucan, I.A., Moll, M., Kavraki, L.E.: The Open Motion Planning Library. *IEEE Robotics & Automation Magazine* **19**(4), 72–82 (December 2012). <https://doi.org/10.1109/MRA.2012.2205651>, <http://ompl.kavrakilab.org>
21. Tallamraju, R., Sripada, V., Karlapalem, K.: A multi-agent control algorithm for failure resilience and energy reduction in multi-wheeled payload transport platforms (2016)
22. Traub, L.W.: Calculation of constant power lithium battery discharge curves. *Batteries* **2**(2), 17 (2016)
23. Vergnano, A., Thorstensson, C., Lennartson, B., Falkman, P., Pellicciari, M., Leali, F., Biller, S.: Modeling and optimization of energy consumption in cooperative multi-robot systems. *IEEE Transactions on Automation Science and Engineering* **9**(2), 423–428 (2012)
24. Wang, Z., Schwager, M.: Multi-robot manipulation without communication. In: *Distributed Autonomous Robotic Systems*, pp. 135–149. Springer (2016)
25. Yang, X., Watanabe\*, K., Izumi, K., Kiguchi, K.: A decentralized control system for cooperative transportation by multiple non-holonomic mobile robots. *International Journal of Control* **77**(10), 949–963 (2004)
26. Zebrowski, P., Vaughan, R.T.: Recharging robot teams: A tanker approach. In: *Advanced Robotics, 2005. ICAR'05. Proceedings., 12th International Conference on*. pp. 803–810. IEEE (2005)
27. Zebrowski, P., Litus, Y., Vaughan, R.T.: Energy efficient robot rendezvous. In: *Computer and Robot Vision, 2007. CRV'07. Fourth Canadian Conference on*. pp. 139–148. IEEE (2007)